Chaotic Phenomena and Fractional-Order Dynamics in the Trajectory Control of Redundant Manipulators

FERNANDO B. M. DUARTE
Department. of Mathematics, School of Technology, Polytechnic Institute of Viseu, Campus Politécnico, 3504-510 Viseu, Portugal, email: fduarte@mat.estv.ipv.pt

J. A. TENREIRO MACHADO
Dept. of Electrical Engineering, Institute of Engineering, Polytechnic Institute of Porto R. Dr.António Bernardino Almeida, 4200-072 Porto, Portugal, email: jtm@dee.isep.ipp.pt

Abstract. Redundant manipulators have some advantages when compared with classical arms because they allow the trajectory optimization, both on the free space and on the presence of obstacles, and the resolution of singularities. For this type of arms the proposed kinematic control algorithms adopt generalized inverse matrices but, in general, the corresponding trajectory planning schemes show important limitations. Motivated by these problems this paper studies the chaos revealed by the pseudoinverse-based trajectory planning algorithms, using the theory of fractional calculus.

Keywords: Planar manipulators, Redundant, Chaos, Fractional calculus

1. Introduction

This paper discusses a fractional calculus perspective in the study of the trajectory control of redundant manipulators and establishes a connection between the theory of fractional order dynamical systems, chaotic phenomena, fractals and robotics.

Fractional calculus goes back to the beginning of the theory of differential calculus but its inherent complexity postponed the application of the associated concepts. Nevertheless, in the last decade the progress in the areas of chaos and fractals revealed subtle relationships with the fractional calculus leading to an increasing interest in the development of the new paradigm. In the area of automatic control some work has been carried out but the proposed algorithms are still in a preliminary phase of establishment.

On the other hand, the area of robotics has been developed since the seventies and researchers have recognized that the addition of extra degrees of freedom (*dof*) to form a

redundant robot overcomes the functional limitations of conventional non-redundant manipulators. However, the kinematic-based redundancy approaches that have been proposed cannot protect against chaotic-like joint motions and high transients.

Having these ideas in mind, the paper is organized as follows. Section 2 develops the formalisms for the fractional calculus and matrix generalized inverses. Section 3 introduces the fundamental issues for the modeling of redundant manipulators. Section 4 analyses the resulting chaotic phenomena revealed by the trajectory planning algorithms. Finally, section 5 draws the main conclusions.

2. Fundamental Aspects

This section introduces the fundamental mathematical aspects of the theories of fractional calculus and matrix generalized inverses.

2.1. Fractional calculus

Fractional calculus is a natural extension of the classical mathematics. In fact, since the beginning of the theory of differential and integral calculus, mathematicians such as Euler and Liouville investigated their ideas on the calculation of non-integer order derivatives and integrals. Nevertheless, in spite of the work that has been done in the area, the application of fractional derivatives and integrals (*FDI*s) has been scarce until recently. In the last years, the advances in the theory of chaos revealed profound relations with *FDI*s, motivating a renewed interest in this field.

The basic aspects of the fractional calculus theory, the study of its properties and research results can be addressed in references [1-13]. In what concerns the application of *FDI* concepts we can mention a large volume of research about viscoelasticity/damping [14-29] and chaos/fractals [30-32]. However, other scientific areas are currently paying attention to the new concepts and we can refer the adoption of *FDI*s in biology [33], electronics [34], signal processing [35-36], system identification [37-39], diffusion and wave propagation [40-42], percolation [43], modelling and identification [44-45], chemistry [46-47] and automatic control [48-54]. This work is still giving its first steps and, consequently, many aspects remain to be investigated.

Since the foundation of the differential calculus the generalization of the concept of derivative and integral to a non-integer order α has been the subject of several approaches.

Due to this reason there are various definitions of *FDI*s (Table I) which are proved to be equivalent.

Table I Definitions of *FDI*s.

Liouville	$\left(I_c^{\alpha}\varphi\right)(x)=\frac{1}{\Gamma(\alpha)}\int_{-\infty}^{x}\frac{\varphi(t)}{(x-t)^{1-\alpha}}dt,\ -\infty<x<+\infty$ $\left(D_c^{\alpha}f\right)(x)=\frac{1}{\Gamma(1-\alpha)}\frac{d}{dx}\int_{-\infty}^{x}\frac{f(t)}{(x-t)^{\alpha}}dt,\ -\infty<x<+\infty$
Riemann-Liouville	$\left(I_{a+}^{\alpha}\varphi\right)(x)=\frac{1}{\Gamma(\alpha)}\int_{a}^{x}\frac{\varphi(t)}{(x-t)^{1-\alpha}}dt,\ a<x$ $\left(D_{a+}^{\alpha}f\right)(x)=\frac{1}{\Gamma(1-\alpha)}\frac{d}{dx}\int_{a}^{x}\frac{f(t)}{(x-t)^{\alpha}}dt,\ a<x$
Hadamard	$\left(I_{+}^{\alpha}\varphi\right)(x)=\frac{1}{\Gamma(\alpha)}\int_{0}^{x}\frac{\varphi(t)}{t[\ln(t/x)]^{1-\alpha}}dt,\ x>0,\ a>0$ $\left(D_{a+}^{\alpha}f\right)(x)=\frac{\alpha}{\Gamma(1-\alpha)}\int_{0}^{x}\frac{f(x)-f(t)}{t[\ln(x/t)]^{1+\alpha}}dt$
Grünwald-Letnikov	$\left(I_{a+}^{\alpha}\varphi\right)(x)=\frac{1}{\Gamma(\alpha)}\lim_{h\to+0}\left[h^{\alpha}\sum_{j=0}^{\left[\frac{x-a}{h}\right]}\frac{\Gamma(\alpha+j)}{\Gamma(j+1)}\varphi(x-jh)\right]$
Caputo	$D_{*}^{\alpha}f(t)=\begin{cases}\frac{1}{\Gamma(m-\alpha)}\int_{0}^{t}\frac{f^{(m)}(\tau)}{(t-\tau)^{\alpha+1-m}}d\tau,\ m-1<\alpha<m\\ \frac{d^{m}}{dt^{m}}f(t),\ m=\alpha\end{cases}$
Marchaud	$\left(D_{+}^{\alpha}f\right)(x)=\frac{\alpha}{\Gamma(1-\alpha)}\int_{-\infty}^{x}\frac{f(x)-f(t)}{(x-t)^{1+\alpha}}dt$
Fourier	$F\left\{I_{\pm}^{\alpha}\varphi\right\}=F\{\varphi\}/(\pm j\omega)^{\alpha},\ 0<\mathrm{Re}(\alpha)<1$ $F\left\{D_{\pm}^{\alpha}\varphi\right\}=(\pm j\omega)^{\alpha}F\{\varphi\},\ \mathrm{Re}(\alpha)\geq 0$
Laplace	$L\left\{I_{0+}^{\alpha}\varphi\right\}=L\{\varphi\}/s^{\alpha},\ \mathrm{Re}(\alpha)>0$ $L\left\{D_{0+}^{\alpha}\varphi\right\}=s^{\alpha}L\{\varphi\},\ \mathrm{Re}(\alpha)\geq 0$

Nevertheless, from the control point of view some definitions seem more attractive, namely when thinking in a real-time calculation. The Laplace/Fourier definition for a

derivative of order $\alpha \in \mathbb{C}$ is a 'direct' generalization of the classical integer-order scheme with the multiplication of the signal transform by the $s/j\omega$ operator. In what concerns automatic control theory this means that frequency-based analysis methods have a straightforward adaptation to *FDI*s.

Consider the elemental control system represented in Figure 1 (with $1 < \alpha < 2$) with transfer function $G(s) = Ks^{-\alpha}$ in the forward path. The open-loop Bode diagrams (Figure 2) of amplitude and phase have a slope of -20α *dB*/*dec* and a constant phase of $-\alpha\pi/2$ *rad*, respectively. Therefore, the closed-loop system has a constant phase margin of $\pi(1 - \alpha/2)$ *rad*, that is, independent of the system gain *K*. Likewise, this important property is also revealed through the root-locus depicted in Figure 3. For example, when $1 < \alpha < 2$ the root-locus follows the relation $\pi - \pi/\alpha = \cos^{-1}\zeta$, where ζ is the damping ratio, independently of the system gain *K*.

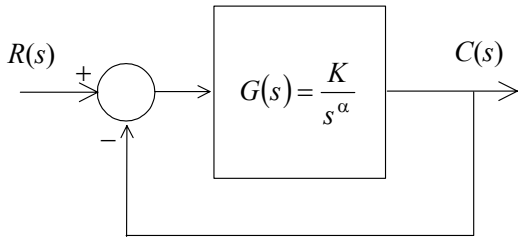

Figure 1 Block diagram for an elemental feedback control system of fractional order α.

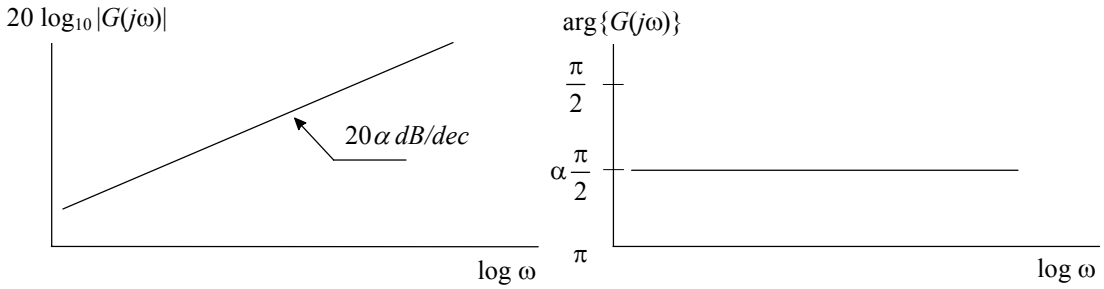

Figure 2 Open-loop Bode diagrams of amplitude and phase for a system of fractional order $1 < \alpha < 2$.

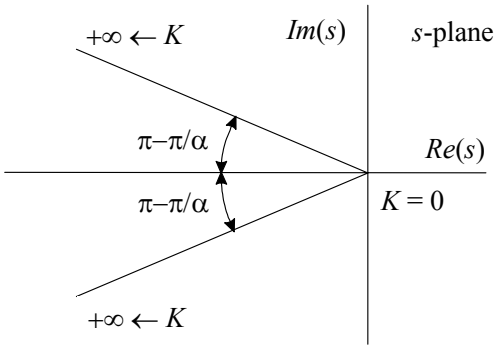

Figure 3 Root locus for a feedback control system of fractional order $1 < \alpha < 2$.

The implementation of *FDI*s based on the Laplace/Fourier definition adopts the frequency domain and requires an infinite number of poles and zeros obeying a recursive relationship [48, 49]. Nevertheless, this approach has several drawbacks. In a real approximation the finite number of poles and zeros yields a ripple in the frequency response and a limited bandwidth. Moreover, the digital conversion of the scheme requires further steps and additional approximations making it difficult to analyze the final algorithm. The method is restricted to cases where a frequency response is well known and, in other circumstances, problems occur for its implementation. An alternative approach is based on the concept of fractional differential of order α. The Grünwald-Letnikov definition of a derivative of fractional order α of the signal $x(t)$, $D^{\alpha}[x(t)]$, motivated an approximation based on a n-term truncated series in the discrete-time domain, that in z-transform is given by [50-52]:

$$Z\left\{D^{\alpha}\left[x(t)\right]\right\} \approx \left[\frac{1}{T^{\alpha}}\sum_{k=0}^{n}\frac{(-1)^{k}\,\Gamma(\alpha+1)}{k!\,\Gamma(\alpha-k+1)}z^{-k}\right]X(z) = Trunc_{n}\left\{\left(\frac{1-z^{-1}}{T}\right)^{\alpha}\right\}X(z) \qquad (1)$$

An important property revealed by the Grünwald-Letnikov definition and aproximation (1) is that while an integer-order derivative implies simply a finite series, the fractional-order derivative requires an infinite number of terms. This means that integer derivatives are ‘local’ operators in opposition with fractional derivatives that have, implicitly, a ‘memory’ of all past events.

2.2. Generalized inverses

This subsection addresses the generalization of the concept on matrix inversion.

For $\mathbf{A} \in \Re^{m \times n}$ and $\mathbf{X} \in \Re^{n \times m}$, the following relations are used to define a generalized inverse $\mathbf{A}^-$, a reflexive generalized inverse $\mathbf{A}_r^-$ and a pseudoinverse $\mathbf{A}^\#$:

$$\mathbf{AXA} = \mathbf{A} \tag{2}$$

$$\mathbf{XAX} = \mathbf{X} \tag{3}$$

$$(\mathbf{AX})^T = \mathbf{AX} \tag{4}$$

$$(\mathbf{XA})^T = \mathbf{XA} \tag{5}$$

Conditions (2) through (5) are called the *Penrose conditions*. A *generalized inverse* of matrix $\mathbf{A} \in \Re^{m \times n}$ is a matrix $\mathbf{X} = \mathbf{A}^- \in \Re^{n \times m}$ satisfying condition (2). On the other hand, a *reflexive generalized inverse* of matrix $\mathbf{A} \in \Re^{m \times n}$ is a matrix $\mathbf{X} = \mathbf{A}_r^- \in \Re^{n \times m}$ satisfying both conditions (2) and (3). Finally, *a pseudoinverse* of a matrix $\mathbf{A} \in \Re^{m \times n}$ (so-called *Moore-Penrose inverse*) is a matrix $\mathbf{X} = \mathbf{A}^\# \in \Re^{n \times m}$ satisfying conditions (2) through (5) [55-58].

The generalized inverse is not unique and, in general, if $\mathbf{A}^-$ is a particular matrix satisfying (2), then all the generalized inverse of matrix **A** are given by (6) where **Y** varies overall possible $n \times m$ matrices:

$$\mathbf{A}^- + \mathbf{Y} - \mathbf{A}^- \mathbf{AYAA}^- \tag{6}$$

Suppose that **A** has rank r and that its rows and columns have been permuted to make the leading $r \times r$ submatrix non-singular. Therefore, to compute a generalized inverse of **A**, we must apply row operations to the augmented matrix $\mathbf{A}_a = [\mathbf{A}, \mathbf{I}_m]$ (assuming $m \geq n$) to reduce it to the form [**B**, **C**] where:

$$\mathbf{B} = \begin{bmatrix} \mathbf{I}_r & \mathbf{B}_1 \\ 0 & 0 \end{bmatrix} \tag{7}$$

is $m \times n$. Then, the first n rows of **C** form a generalized inverse of **A**. If $m < n$ the procedure can be applied to $\mathbf{A}^T$, leading to $\mathbf{A}^-$.

For a given $\mathbf{A} \in \Re^{m \times n}$ the pseudoinverse $\mathbf{A}^{\#} \in \Re^{n \times m}$ exists and is unique, whereas $\mathbf{A}_r^-$ and $\mathbf{A}^-$ are not necessarily unique. Let the sets of $\mathbf{A}^-$, $\mathbf{A}_r^-$ and $\mathbf{A}^{\#}$ be S^-, S_r^- and $S^{\#}$, respectively. Then, the following inclusion relation holds:

$$S^{\#} \subset S_r^- \subset S^- \tag{8}$$

The following properties are analogous to those of the ordinary inverse:

i) $\left(\mathbf{A}^{\#}\right)^{\#} = \mathbf{A}$

ii) $\left(\mathbf{A}^T\right)^{\#} = \left(\mathbf{A}^{\#}\right)^T$

iii) $\mathbf{A}^{\#} = \left(\mathbf{A}^T\mathbf{A}\right)^{\#}\mathbf{A}^T = \mathbf{A}^T\left(\mathbf{A}\mathbf{A}^T\right)^{\#}$.

For a matrix $\mathbf{A} \in \Re^{m \times n}$:

i) If $m < n$ and $r(\mathbf{A}) = m$, then $\mathbf{A}\mathbf{A}^T$ is nonsingular and

$$\mathbf{A}^{\#} = \mathbf{A}^T\left(\mathbf{A}\mathbf{A}^T\right)^{-1} \tag{9}$$

ii) If $m > n$ and $r(\mathbf{A}) = n$, then $\mathbf{A}^T\mathbf{A}$ is nonsingular and

$$\mathbf{A}^{\#} = \left(\mathbf{A}^T\mathbf{A}\right)^{-1}\mathbf{A}^T \tag{10}$$

iii) If $m = n$ and $r(\mathbf{A}) = n$ then

$$\mathbf{A}^{\#} = \left(\mathbf{A}\right)^{-1} \tag{11}$$

The matrices $\mathbf{A}^{\#}\mathbf{A}$, $\mathbf{A}\mathbf{A}^{\#}$, $\mathbf{I} - \mathbf{A}^{\#}\mathbf{A}$ and $\mathbf{I} - \mathbf{A}\mathbf{A}^{\#}$, where **I** represents an identity matrix of appropriate dimension, are all idempotent and symmetric. If $\mathbf{A} \in \Re^{n \times n}$ is symmetric and idempotent then, for any matrix $\mathbf{B} \in \Re^{m \times n}$, the following condition holds:

$$\mathbf{A}\left(\mathbf{B}\mathbf{A}\right)^{\#} = \left(\mathbf{B}\mathbf{A}\right)^{\#} \tag{12}$$

If $\mathbf{A} \in \Re^{m \times n}$ the matrix $\mathbf{A}^T\mathbf{A}$ is non-negative with real non-negative eigenvalues $\lambda_1, \lambda_2, \cdots, \lambda_n \quad (\lambda_1 \geq \lambda_2 \geq \cdots \geq \lambda_n \geq 0)$ and the singular values of $\mathbf{A}$ are $\sigma_i = \sqrt{\lambda_i},\ i = 1, 2, ..., \min(m,n)$ with $\sigma_1 \geq \sigma_2 \geq \cdots \geq \sigma_{\min(m,n)} \geq 0$. Then there are two orthogonal matrices $\mathbf{U} = (\mathbf{u}_1, \mathbf{u}_2, \cdots, \mathbf{u}_m) \in \Re^{mxm}$ and $\mathbf{V} = (\mathbf{v}_1, \mathbf{v}_2, \cdots, \mathbf{v}_n) \in \Re^{nxn}$, such that $\mathbf{A}$ is represented by $\mathbf{A} = \mathbf{U}\Sigma\mathbf{V}^T$, where $\mathbf{\Sigma} \in \Re^{mxn}$ is given by:

$$\mathbf{\Sigma} = \begin{bmatrix} \sigma_1 & & 0 \\ & \ddots & \\ 0 & & \sigma_n \\ \hline & 0 & \end{bmatrix} \ if\ m \geq n \quad \text{or} \quad \mathbf{\Sigma} = \left[\begin{array}{ccc:c} \sigma_1 & & 0 & \\ & \ddots & & 0 \\ 0 & & \sigma_n & \end{array}\right] \text{ if } m < n \tag{13}$$

When $\mathbf{A}$ is decomposed by the Singular Value Decomposition (SVD), its pseudoinverse $\mathbf{A}^{\#}$ is represented by

$$\mathbf{A}^{\#} = \mathbf{V}\Sigma^{\#}\mathbf{U}^T, \quad \mathbf{\Sigma}^{\#} = \left[\begin{array}{ccc:c} \sigma_1^{-1} & 0 & 0 & \\ 0 & \ddots & 0 & 0 \\ 0 & 0 & \sigma_p^{-1} & \\ \hline & 0 & & 0 \end{array}\right] \tag{14}$$

where p is the number of non-zero singular values.

When the matrix $\mathbf{A} \in \Re^{m \times n}$ is full rank the pseudoinverse is computed using the regular inverse of a non-singular matrix. From (9) and (10) the pseudoinverse is computed as follows:

i) If $m < n$ and $r(\mathbf{A}) = m$ then

$$\mathbf{A}^{\#} = \mathbf{A}^T\left(\mathbf{A}\mathbf{A}^T\right)^{-1} \tag{15}$$

ii) If $m > n$ and $r(\mathbf{A}) = n$ then

$$\mathbf{A}^{\#} = \left(\mathbf{A}\mathbf{A}^T\right)^{-1}\mathbf{A}^T \tag{16}$$

From (11) $\mathbf{A}^{\#} = \mathbf{A}^{-1}$, if $m = n$ and $r(\mathbf{A}) = m$.

3. Modelling of Redundant Manipulators

This section addresses the concepts associated with the generalization of classical manipulating structures in the perspective of introducing *dof* to form redundant robots.

A kinematically redundant manipulator is a robotic arm possessing more *dof* than those required to establish an arbitrary position and orientation of the end effector (Figure 4). Redundant manipulators offer several potential advantages over non-redundant arms. In a workspace with obstacles, the extra *dof* can be used to move around or between obstacles and, thereby, to manipulate in situations that otherwise would be inaccessible.

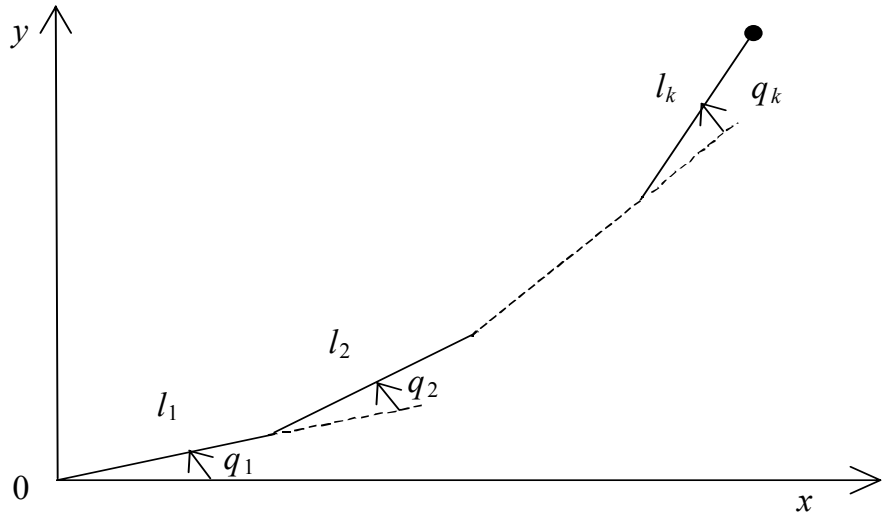

Figure 4 A *kR* planar redundant manipulator.

When a manipulator is redundant it is anticipated that the inverse kinematics admits an infinite number of solutions. This implies that, for a given location of the manipulator's end effector, it is possible to induce a self-motion of the structure without changing the location of the gripper. Therefore, redundant manipulators can be reconfigured to find better postures for an assigned set of task requirements but, on the other hand, have a more complex structure requiring sophisticated control algorithms.

We consider a manipulator with *n dof* whose joint variables are denoted by $\mathbf{q} = [q_1, q_2, ..., q_n]^T$ and a class of operational tasks described by *m* variables $\mathbf{x} = [x_1, x_2, ..., x_m]^T$, $m < n$. The relation between the joint vector **q** and the manipulation vector **x** corresponds to the direct kinematics:

$$\mathbf{x} = f(\mathbf{q}) \tag{17}$$

Differentiating (17) with respect to time yields:

$$\dot{\mathbf{x}} = \mathbf{J}(\mathbf{q})\dot{\mathbf{q}} \tag{18}$$

where $\dot{\mathbf{x}} \in \Re^m$, $\dot{\mathbf{q}} \in \Re^n$ and $\mathbf{J}(\mathbf{q}) = \partial f(\mathbf{q})/\partial \mathbf{q} \in \Re^{m \times n}$. Hence, from (18) it is possible to calculate a $\mathbf{q}(t)$ path in terms of a prescribed trajectory $\mathbf{x}(t)$. A solution in terms of the joint velocities, is sought as:

$$\dot{\mathbf{q}} = \mathbf{K}(\mathbf{q})\dot{\mathbf{x}} \tag{19}$$

where $\mathbf{K}$ is a suitable $(n \times m)$ control matrix based on the Jacobian matrix:

$$\dot{\mathbf{q}} = \mathbf{J}^{\#}(\mathbf{q})\dot{\mathbf{x}} \tag{20}$$

where $\mathbf{J}^{\#}$ is one of the generalized inverses of the $\mathbf{J}$.

If $\mathbf{J}^{\#}$ is the pseudoinverse, satisfying conditions (2) through (5), it can be easily shown that a more general solution to equation (18) is given by:

$$\dot{\mathbf{q}} = \mathbf{J}^{\#}(\mathbf{q})\dot{\mathbf{x}} + \left[\mathbf{I} - \mathbf{J}^{\#}(\mathbf{q})\mathbf{J}(\mathbf{q})\right]\dot{\mathbf{q}}_0 \tag{21}$$

where $\mathbf{I}$ is $(n \times n)$ identity matrix and $\dot{\mathbf{q}}_0$ is a $(m \times 1)$ arbitrary joint velocity vector.

Solution (21) is composed of two terms: the first term is relative to minimum norm joint velocities and the second term (the *homogeneous solution*) attempts to satisfy the additional constraints specified by $\dot{\mathbf{q}}_0$. The expression $\mathbf{I} - \mathbf{J}^{\#}(\mathbf{q})\mathbf{J}(\mathbf{q})$ is a matrix that allows the projection of $\dot{\mathbf{q}}_0$ in the null space of $\mathbf{J}$. A direct consequence is that it is possible to generate internal motions that reconfigure the manipulator structure without changing the gripper position and orientation [59-62].

We assume that the following condition is satisfied:

$$\text{Max}[\text{rank } \{\mathbf{J}(\mathbf{q})\}] = m \tag{22}$$

Failing to satisfy this condition usually means that the selection of manipulation variables is redundant and the number of these variables m can be reduced. When condition (22) is satisfied, we say that the degree of redundancy of the manipulator is $n-m$. If, for some $\mathbf{q}$ we verify that:

$$\text{rank}\,\{\mathbf{J}(\mathbf{q})\} < m \tag{23}$$

then the manipulator is in a singular state. This state is not desirable because, in this region of the trajectory, the manipulating ability is very limited. Based on these concepts, to analyze and quantify the problem of object manipulation it was proposed [63] the index $\mu = \left[\det\left(\mathbf{J}\mathbf{J}^T\right)\right]^{1/2}$ as a measure of the manipulability at state $\mathbf{q}$.

In the closed-loop pseudoinverse's method (CLP) the joint positions can be computed through the time integration of the velocities (18) according with the block diagram depicted in Figure 5.

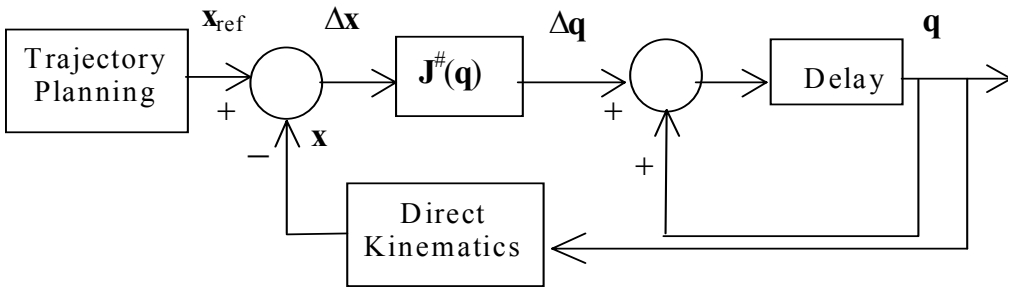

Figure 5 Block diagram of the closed-loop inverse kinematics algorithm with the pseudoinverse.

An aspect revealed by the CLP is that repetitive trajectories in the operational space do not lead to periodic trajectories in the joint space [64, 65]. This is an obstacle for the solution of many tasks because the resultant robot configurations have similarities with those of a chaotic system.

To overcome this problem other alternatives methods for trajectory planning were proposed, namely by augmenting the Jacobian or by introducing optimization criteria (so that it becomes of order $n \times n$). For example, the Open-Loop Manipulability (OLM) optimization method [66, 67] gives superior results in what concerns a μ-optimization and the repeatability. Nevertheless, clear conclusions both about the most adequate optimization method and the nature of the phenomena involved when using $\mathbf{J}^{\#}$ are still lacking.

In this paper we analyse the phenomena involved in the adoption of the CLP algorithm. We consider *k*-link planar manipulators and, in this case, the direct kinematics and the Jacobian have simple recursive expressions:

$$\begin{bmatrix} x \\ y \end{bmatrix} = \begin{bmatrix} l_1C_1 + l_2C_{12} + l_3C_{123} + \cdots + l_kC_{12\ldots k} \\ l_1S_1 + l_2S_{12} + l_3S_{123} + \cdots + l_kS_{12\ldots k} \end{bmatrix} \qquad (24\text{ -a})$$

$$\mathbf{J} = \begin{bmatrix} -l_1S_1 - l_2S_{12} - \cdots - l_kS_{1\cdots k} & \cdots & -l_kS_{1\cdots k} \\ l_1C_1 + l_2C_{12} + \cdots + l_kC_{1\cdots k} & \cdots & l_kC_{1\cdots k} \end{bmatrix} \qquad (24\text{ -b})$$

where l_i is the length of link *i*, $S_{i\cdots k} = Sin(q_i + \cdots + q_k)$ and $C_{i\cdots k} = Cos(q_i + \cdots + q_k)$. During all the experiments, it is considered $\Delta t = 0.001\,\text{sec}$, $l_T = l_1 + l_2 + \ldots + l_k = 3\ m$, $l_1 = l_2 = \ldots = l_k$, $m_T = m_1 + m_2 + \ldots + m_k = 3$ kg and $m_1 = \ldots = m_k$.

4. The Chaotic Responses of the Pseudoinverse Algorithm Control of Redundant Manipulators

This section analyses the chaotic behaviour of redundant manipulators with the CLP algorithm. In this line of thought, it is organized in four sub-sections corresponding to complementary study perspectives namely, the fractal dimension of the phase plane trajectories, the statistical distribution of the robot joint variables, the CLP frequency response and the Fourier transform of the robot joint velocities, for several distinct working conditions.

4.1. Fractal dimension

It is well known that the CLP algorithm leads to unpredictable arm configurations with responses similar to those of a chaotic system [68-75]. For example, Figures 6–11 depict the phase-plane joint trajectories for the 3*R*-robot positions and torques, respectively, when repeating a circular motion with frequency $\omega_0 = 3$ *rad/sec*, center at $r = [x^2+y^2]^{½} = 1$ *m* and radius $\rho = 0.1$ *m*. Besides the position and velocity drifts, leading to different trajectory loops, we have points that are 'avoided'. Such points correspond to arm configurations where several links are aligned. This characteristic is inherent to $\mathbf{J}^{\#}$ because the 3*R*-robot was tested both under open-loop and closed-loop control, leading to the same type of chaotic behavior. In order to gain further insight into the pseudoinverse nature, the robots under investigation were required to follow the cartesian repetitive circular motion for several

radial distances r and radius ρ. The phase-plane joint trajectories were then analyzed and their fractal dimension estimated through the two methods:

i) Lyapunov dimension

$$\dim_L S = 1 - \frac{\ln \lambda_1}{\ln \lambda_2} \tag{25}$$

where λ_1 and λ_2 are the nonzero real eigenvalues of $\mathbf{JJ}^{\mathrm{T}}$.

ii) standard box-counting dimension

$$\dim_C S = \lim_{\varepsilon \to 0} \frac{\ln N(\varepsilon)}{\ln (1/\varepsilon)} \tag{26}$$

where $N(\varepsilon)$ denotes the smallest number of bi-dimensional boxes of side length ε required in order to completely cover the plot surface S [76-79] .

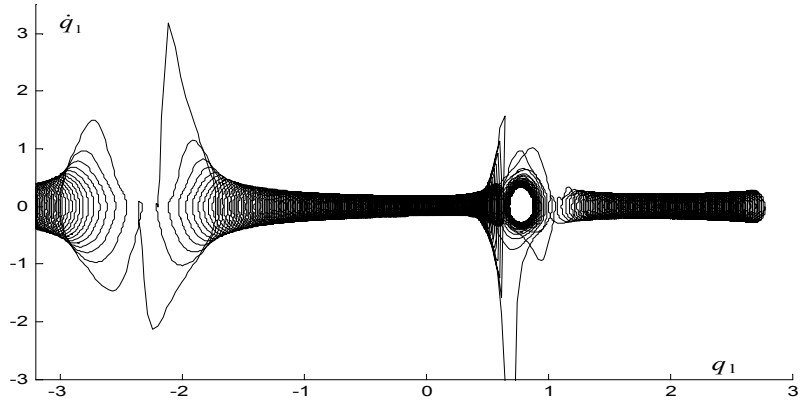

Figure 6 Phase plane trajectory for the 3*R*- robot joint 1 at $r = 1$ *m*, $\rho = 0.1$ *m*, $\omega_0 = 3$ *rad/sec*, $dim_C = 1.62$, $dim_L = 0.88$.

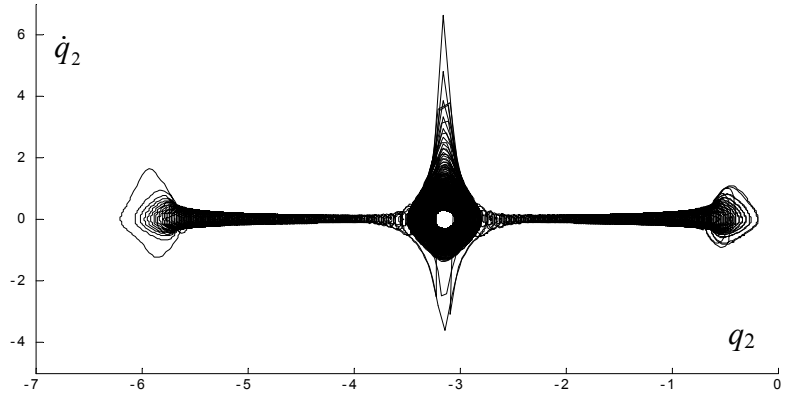

Figure 7 Phase plane trajectory for the 3*R*- robot joint 2 at $r = 1$ *m*, $\rho = 0.1$ *m*, $\omega_0 = 3$ *rad/sec*, $dim_C = 1.60$, $dim_L = 0.88$.

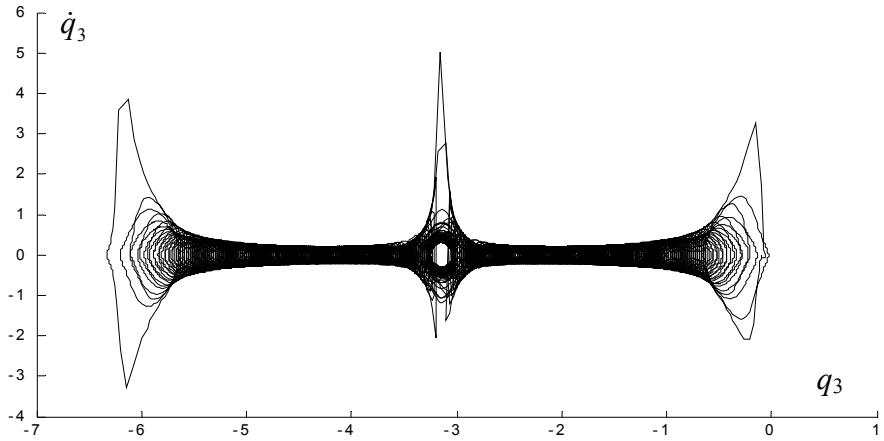

Figure 8 Phase plane trajectory for the 3*R*- robot joint 3 at $r = 1$ *m*, $\rho = 0.1$ *m*, $\omega_0 = 3$ *rad/sec*, $dim_C = 1.63$, $dim_L = 0.88$.

It is clear that the CLP method leads to chaotic responses with fast transients and high accelerations. Applying expressions (25)-(26) to the previous results we get Figures 9-10 revealing that:

- for the CLP method we have $dim_C > 1$ due to the position and velocity drifts, in contrast with the 'standard' case, that is, for non-redundant robot trajectories, where we have $dim_C = 1$.
- dim_C diminishes near the maximum radial distance $r = 3$ *m*.
- for each type of robot (3*R* and 4*R*) dim_C is nearly the same, for all joints.
- As it is known from the chaos theory that, in general, $dim_L \neq dim_C$. Nevertheless, the locus $r = r_s$ ($r_s = 1$ *m* and $r_s = 1.5$ *m* for the 3*R* and 4*R* robots, respectively) seems to be the limit between two distinct regions.
- For $r > r_s$ both the 3*R* and 4*R* robots have, approximately, similar values for dim_L and dim_C .

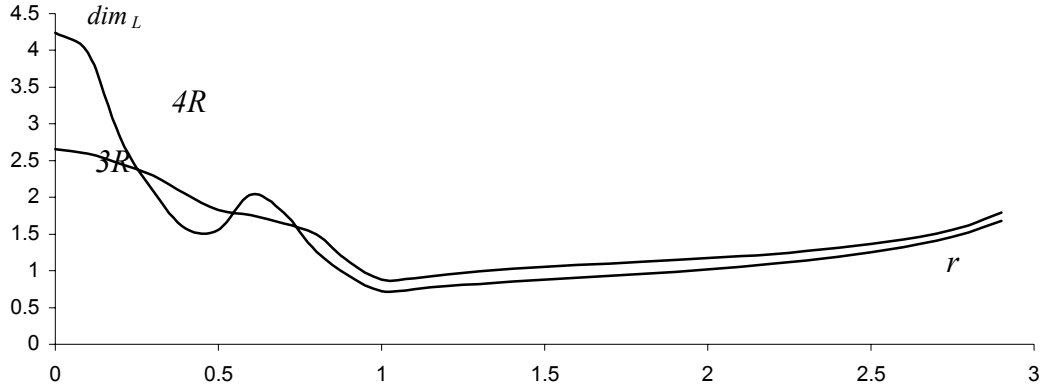

Figure 9 Lyapunov dimension (dim_L) of the kinematic phase-plane *versus* the radial distance r, for the 3R and 4R robots, $\rho = 0.1$ *m* and $\omega_0 = 3$ *rad/sec*.

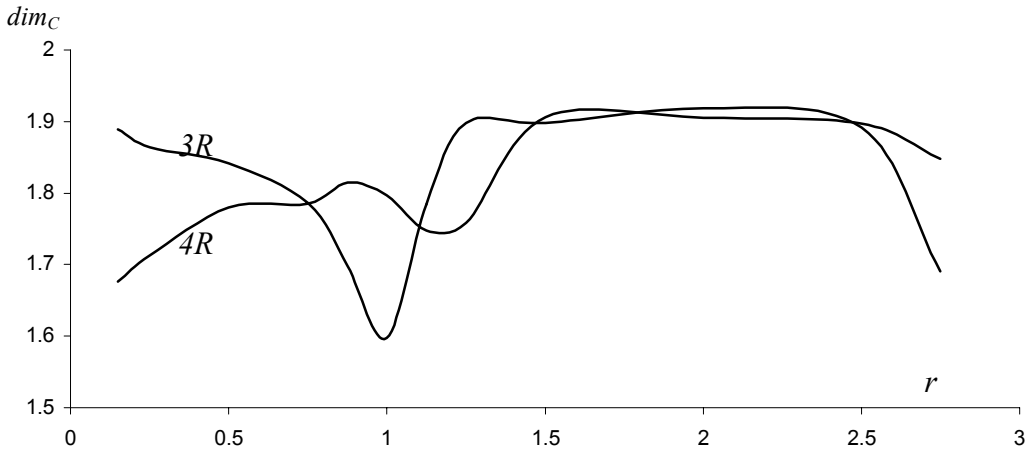

Figure 10 Counting-box dimension (dim_C) of the kinematic phase-plane *versus* the radial distance r, for the 3R and 4R robots, $\rho = 0.1$ *m* and $\omega_0 = 3$ *rad/sec*.

4.2. Statistical distribution of the joint variables

The chaotic motion is due to the $\mathbf{J}^{\#}$ contribution to the manipulator inner motion. Nevertheless, a deeper insight into the nature of this motion must be envisaged. Therefore, several distinct experiments were devised in order to establish the texture of the Jacobian. In a first set of experiments Figures 11 and 12 show the statistical distribution of the joint variables, $\mathbf{q}_i$ (i = 1,2,…,n), versus r for the 3R and 4R robots under the CLP with $\rho = 0$. We conclude that:

- The possible robot configurations have distinct probabilities.
- The histograms for the first axis has distinct characteristics while the other have a similar aspect.
- For the $3R$ and $4R$ robots the singular points $r_s = 1\ m$ and $r_s = 1.5\ m$, respectively, represent the boundary between two distinct regions, namely $0 < r < r_s$ and $r_s < r < l_T$.

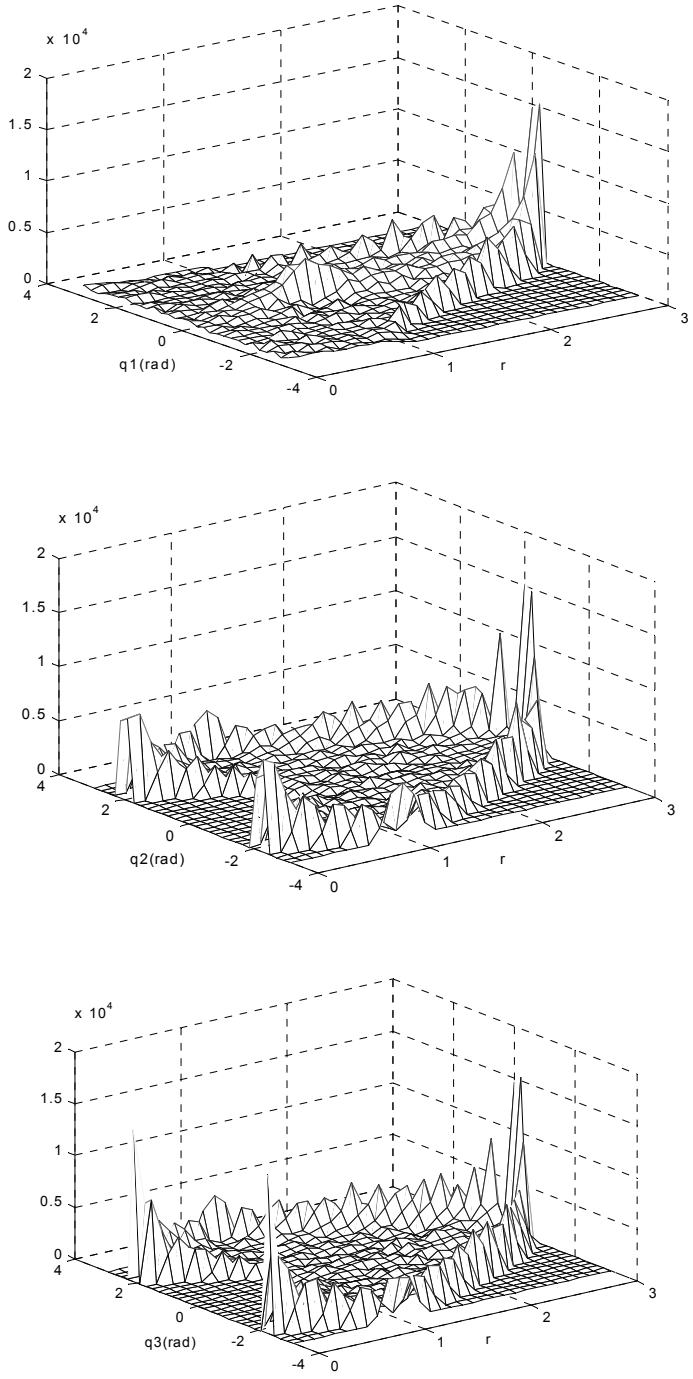

Figure11 Statistical distribution of the $3R$ robot joint positions *vs* the radial distance r for $\rho = 0$. Singular point $r_s = 1\ m$.

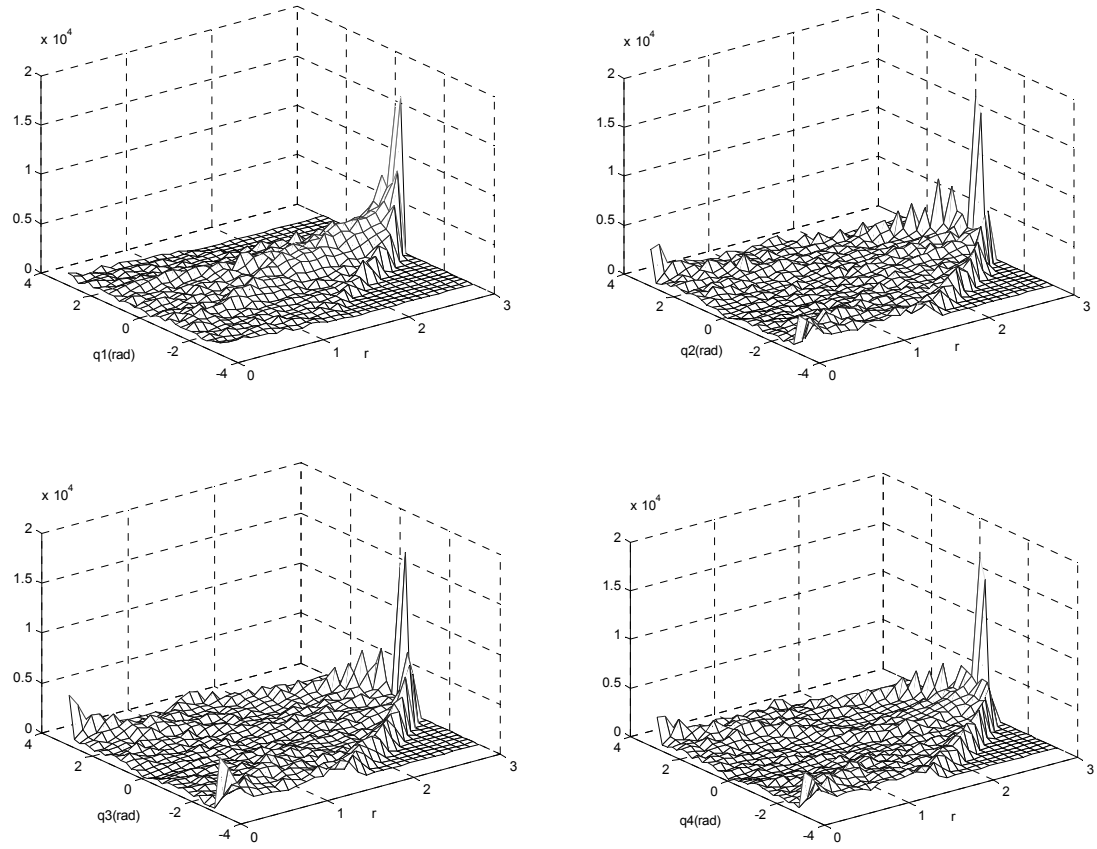

Figure 12 Statistical distribution of the 4*R* robot joint positions *vs* the radial distance *r* for $\rho = 0$. Singular point $r_s = 1.5$ *m*.

4.3. Frequency responses for the CLP method

In another set of experiments the frequency response of the CLP method for the 3*R* and 4*R* robots is computed numerically for a doublet-like exciting signal at $t \in [\ 0.9,\ 1.1]$ *sec* superimposed over the sinusoidal reference.

Figures 13 and 14 depict the 3*R* and 4*R* robots Bode diagrams for $r = 2$ *m* and $\rho \in \{0.10,\ 0.25,\ 0.50,\ 0.75\}$ *m*. It is clear that the transfer matrix for the *MIMO* system (x_{ref}, y_{ref}) $\rightarrow$ (q_1, q_2, q_3) depends strongly on the amplitude of the 'exciting' signal ρ. Moreover, the Bode diagrams reveal that the CLP method presents distinct gains for the joint variables, according with the frequency. This conclusion is consistent with the phase-plane charts, that revealed low frequency drifts, while responding to an higher frequency (ω_0) input signal.

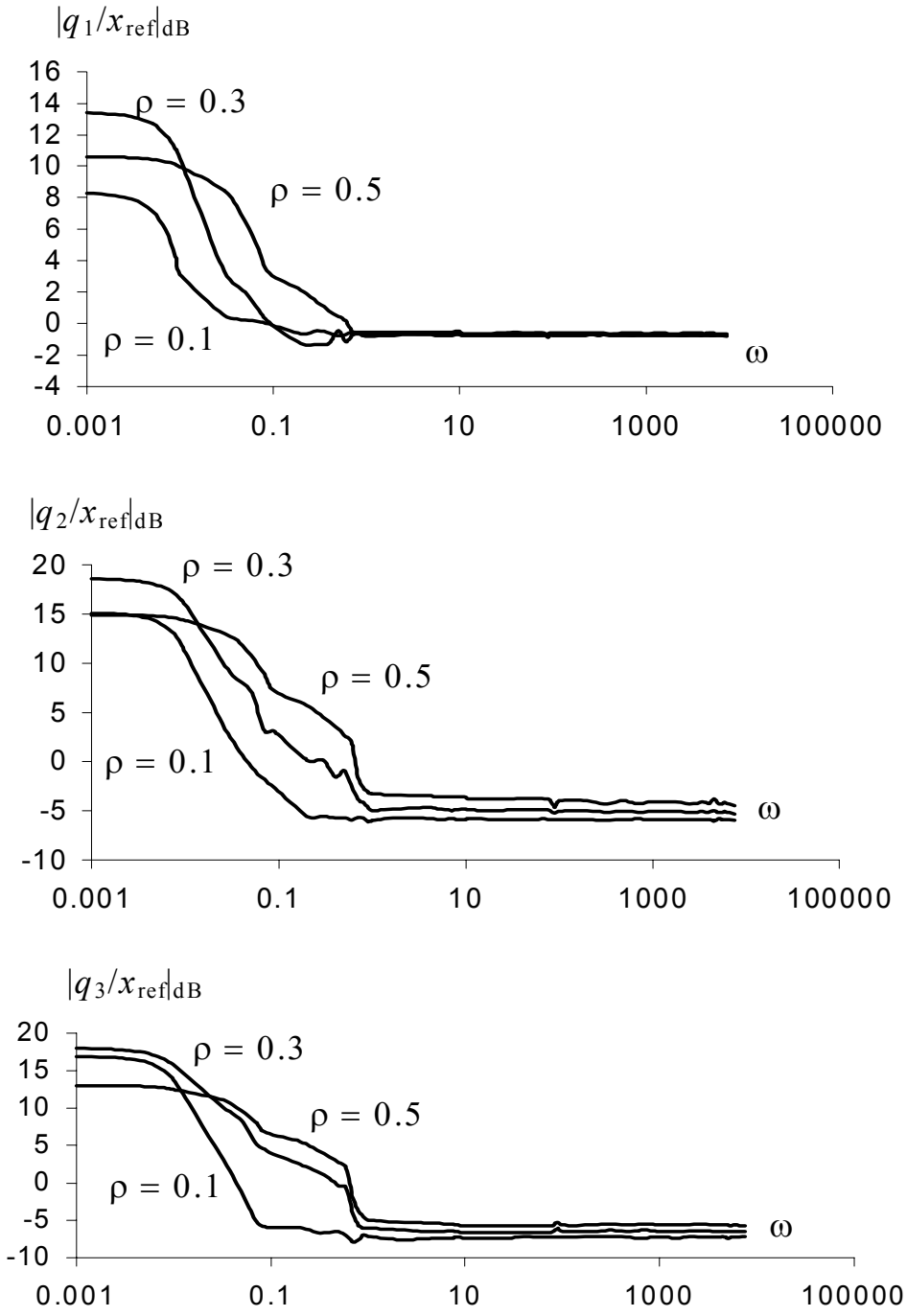

Figure 13 Frequency response of the CLP method for the 3*R* robot, $\omega_0 = 3$ *rad/sec*, $r = 2$ *m*, $\rho \in \{0.10, 0.30, 0.50\}$ *m* and a doublet-like exciting signal.

Table II and III show the parameters for the transfer functions of the type:

$$\frac{Q_i(s)}{X_{ref}(s)} = k\frac{s^{\alpha}+a}{s^{\alpha}+b} \tag{27}$$

for the 3R and 4R robots, respectively. Note that α takes values such that $\alpha \approx 1$.

Table II

Transfer function parameters for the 3*R* robot kinematics under CLP and a doublet-like exciting signal.

	ρ	a	b	k	α
q_1/x_{ref}	0.10	0.01	0.004	0.96	1.09
	0.30	0.03	0.007	0.96	1.07
	0.50	0.18	0.050	0.95	0.89
q_2/x_{ref}	0.10	0.07	0.007	0.50	1.03
	0.30	0.31	0.02	0.55	0.88
	0.50	0.82	0.09	0.61	0.81
q_3/x_{ref}	0.10	0.06	0.004	0.44	1.14
	0.15	0.66	0.04	0.47	0.79
	0.50	0.86	0.10	0.52	0.87

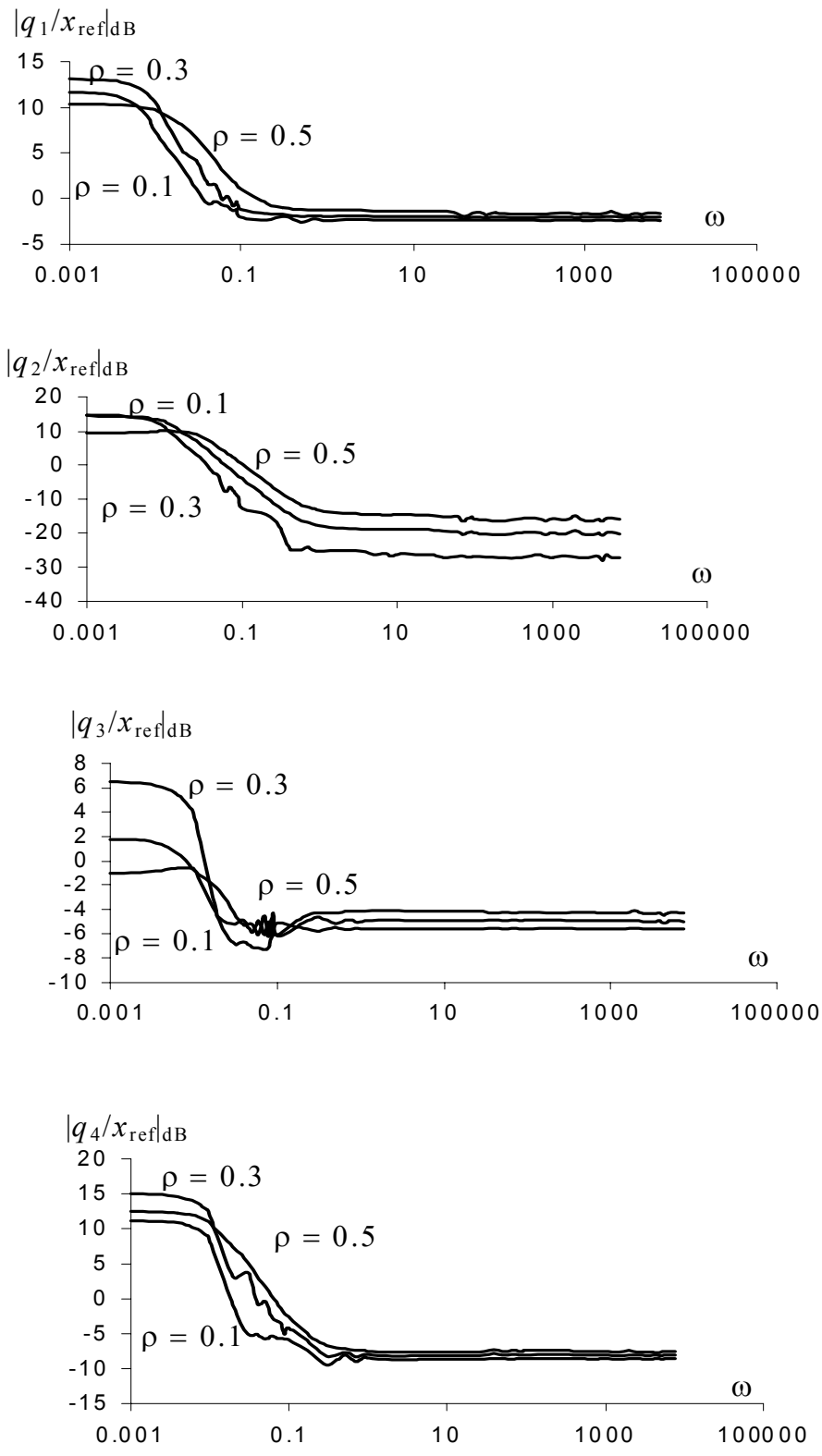

Figure 14 Frequency response of the CLP method for the 4*R* robot, $\omega_0 = 3$ *rad/sec*, $r = 2$ *m*, $\rho \in \{0.10, 0.30, 0.50\}$ *m* and a doublet-like exciting signal.

Table III

Transfer function parameters for the 4*R* robot kinematics under CLP and a doublet-like exciting signal.

	ρ	a	b	k	α
q_1/x_{ref}	0.10	0.04	0.007	0.76	1.02
	0.30	0.05	0.009	0.78	1.02
	0.50	0.12	0.03	0.83	0.93
q_2/x_{ref}	0.10	0.61	0.005	0.04	1.06
	0.30	0.53	0.01	0.10	1.04
	0.50	0.73	0.04	0.16	0.98
q_3/x_{ref}	0.10	0.07	0.04	0.53	0.97
	0.30	0.01	0.006	0.56	1.09
	0.50	0.003	0.001	0.61	1.41
q_4/x_{ref}	0.10	0.04	0.004	0.38	1.12
	0.30	0.08	0.006	0.40	1.07
	0.50	0.20	0.02	0.42	0.91

The other set of experiments addresses also the frequency response but, in this case the exciting signal is white noise distributed throughout the 500-cycle trajectories in order to capture information about the system during all the dynamic evolution. Figures 15 and 16 depict the resulting amplitude Bode gain diagrams.

In this case α takes fractional values (Tables III-IV) in contrast with the previous results. This is due to the memory-time property of *FDIs* because they capture the dynamic phenomena involved during all the time-history of the experiment. For y_{ref} we get the same conclusions.

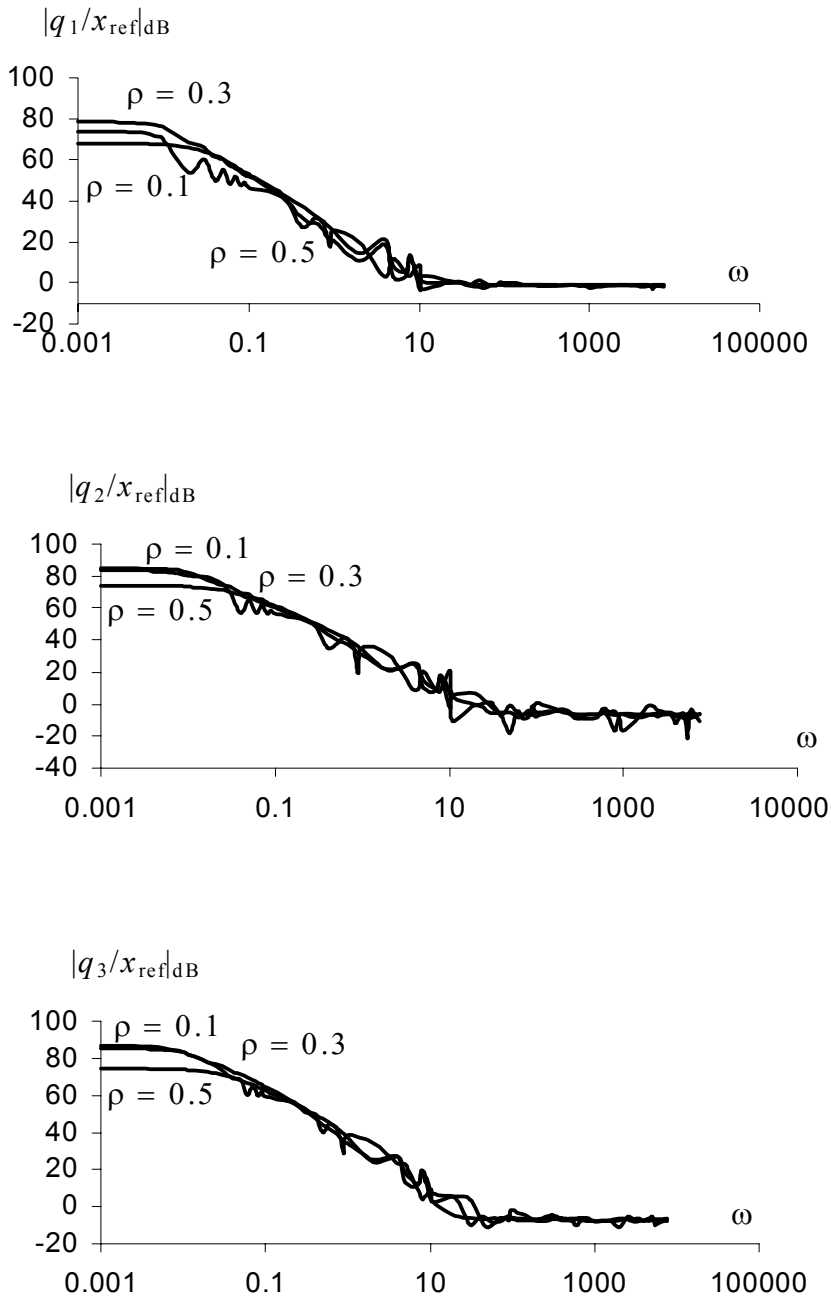

Figure 15 Frequency response of the CLP method for the 3*R* robot, $\omega_0 = 3$ *rad/sec*, $r = 2$ *m*, $\rho \in \{0.10, 0.30, 0.50\}$ *m* and a white noise perturbation during all trajectory.

Tables IV and V show the parameters for the transfer functions of the type (27) for the 3*R* and 4*R* robots kinematics, respectively. Note that, in general, α takes fractional-order values, namely $1.0 < \alpha < 1.4$, in contrast with the results previously obtained for the third set of experiments. This is due to the memory-like property of *FDI*s, in contrast with integer-order derivatives that just capture "local" dynamics.

On the other hand, robot 3*R* seems "more fractional" that robot 4*R*, which seems in accordance with other experiments namely the Figures 17-19 versus Figures 20-23 where the region $0 < r < r_s$ seems "less chaotic" for the 4*R* robot. For y_{ref} we get the same type of conclusions.

Table IV

Transfer function parameters for the 3*R* robot kinematics under CLP and a white noise exciting signal is distributed throughout the 500-cycle trajectories.

	ρ	a	b	k	α
q_1/x_{ref}	0.10	15.8	0.003	0.93	1.13
	0.30	18.8	0.002	0.89	1.32
	0.50	30.3	0.01	0.83	1.23
q_2/x_{ref}	0.10	64.3	0.002	0.47	1.20
	0.30	82.9	0.002	0.43	1.34
	0.50	119.0	0.01	0.43	1.31
q_3/x_{ref}	0.10	101.0	0.002	0.43	1.26
	0.30	120.9	0.003	0.47	1.38
	0.50	130.0	0.01	0.40	1.33

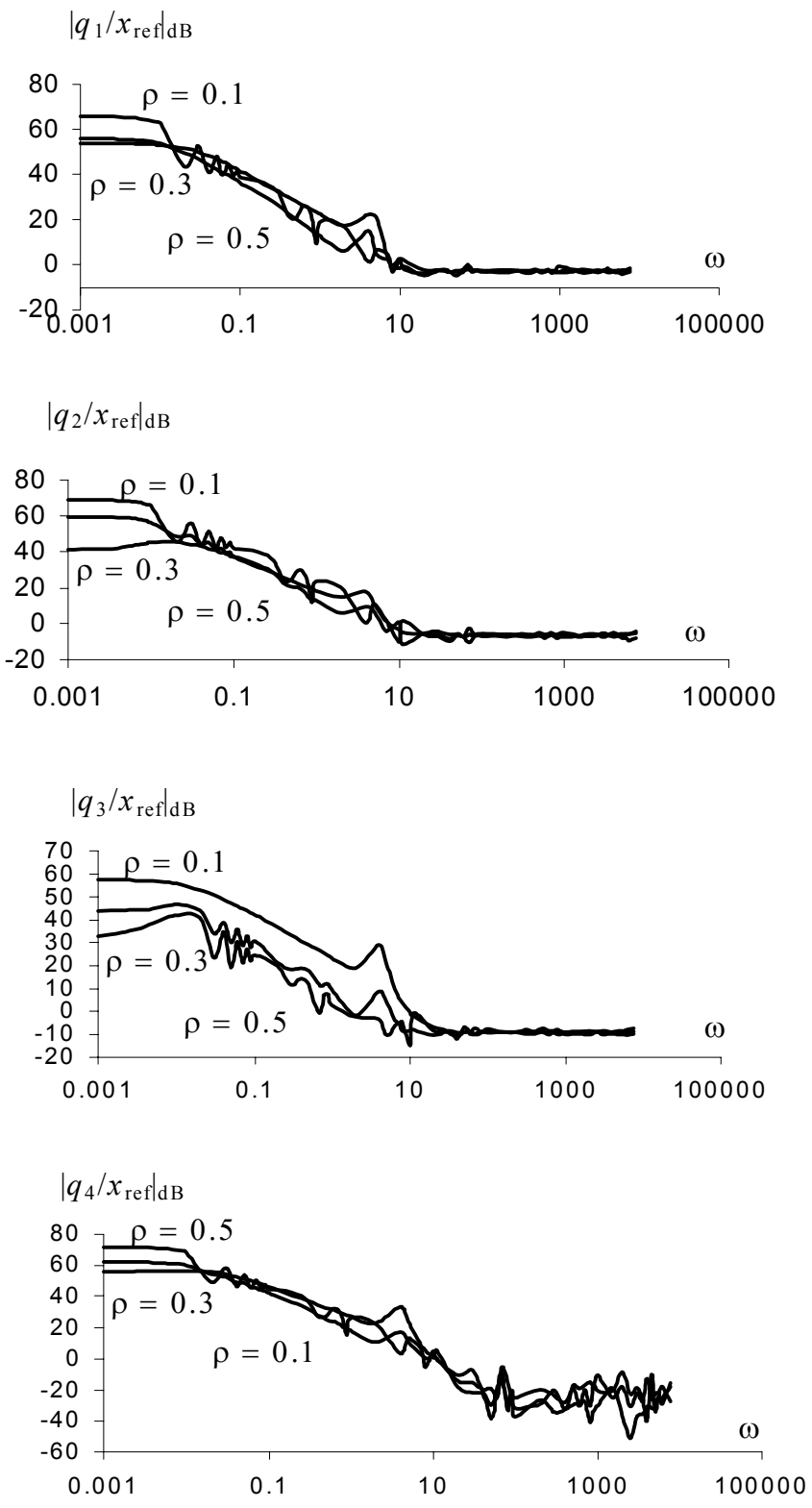

Figure 16 Frequency response of the CLP method for the 4*R* robot , $\omega_0 = 3$ *rad/sec*, $r = 2$ *m*, $\rho \in \{0.10, 0.30, 0.50\}$ *m* and a white noise perturbation during all trajectory.

Table V
Transfer function parameters for the 4*R* robot kinematics under CLP and a white noise exciting signal is distributed throughout the 500-cycle trajectories.

	ρ	a	b	k	α
q_1/x_{ref}	0.10	10.2	0.004	0.75	1.06
	0.30	7.7	0.01	0.77	1.02
	0.50	21.8	0.03	0.66	0.97
q_2/x_{ref}	0.10	139.9	0.003	0.8	1.15
	0.30	116.9	0.007	0.08	1.17
	0.50	263.2	0.03	0.07	1.20
q_3/x_{ref}	0.10	16.7	0.003	0.51	1.13
	0.30	10.6	0.006	0.55	1.08
	0.50	24.8	0.08	0.37	1.01
q_4/x_{ref}	0.10	2.7	0.02	0.36	1.05
	0.30	7.7	0.02	0.40	0.99
	0.50	47.2	0.02	0.31	1.00

4.4. Fourier transform of the robot joint velocities

In the last group of experiments, after elapsing an initial transient, we calculate the Fourier transform of the robot joint velocities for a large number of cycles of circular repetitive motion with frequency $\omega_0 = 3$ *rad/sec*.

Figures 17-23 shows the results for the 3*R* and 4*R* robots versus the radial distance *r,* the center of the circle, with radius $\rho = 0.10$ *m*. Once more we verify that for $0 < r < r_s$ we get a signal energy distribution along all frequencies, while for $r_s < r < 3$ *m* the major part of the signal energy is concentrated at the fundamental and multiple harmonics. Moreover, the DC component, responsible for the position drift, presents distinct values, according to the radial distance *r* and ρ:

$$\left|\dot{q}_i(\omega = 0)\right| = a\rho^d \,/\left(b + r^c\right) \;,\; i=1,2,\ldots,n. \qquad (28)$$

Tables VI and VII show the values of the parameters of equation (28) for the 3*R* and 4*R* robots, respectively.

Table VI
Parameters of the Fourier transform for the DC component of the 3*R* robot joint velocities.

	ρ	*a*	*b*	*c*	*d*
$\dot{q}_1(\omega = 0)$	0.005	480	0.16	3.40	2.10
	0.01	430	0.15	3.30	2.10
	0.05	235	0.16	4.80	1.90
	0.1	465	0.14	4.20	2.20
$\dot{q}_2(\omega = 0)$	0.005	315	0.96	3.20	1.90
	0.01	325	0.94	3.10	1.90
	0.05	385	1.43	3.10	1.90
	0.1	375	1.96	2.20	2.10
$\dot{q}_3(\omega = 0)$	0.005	250	0.73	1.70	1.90
	0.01	245	0.62	1.60	1.90
	0.05	320	1.30	1.90	1.90
	0.1	385	1.93	1.20	2.30

Table VII
Parameters of the Fourier transform for the DC component of the 4*R* robot joint velocities.

	ρ	*a*	*b*	*c*	*d*
$\dot{q}_1(\omega = 0)$	0.005	585	0.10	2.70	2.20
	0.01	510	0.10	2.70	2.20
	0.05	400	0.20	4.40	2.10
	0.1	495	0.05	3.70	2.50
$\dot{q}_2(\omega = 0)$	0.005	295	0.80	2.50	2.00
	0.01	475	0.85	2.50	2.10
	0.05	325	0.45	4.40	2.00
	0.1	200	0.25	2.10	2.20
$\dot{q}_3(\omega = 0)$	0.005	215	0.05	1.90	2.40
	0.01	410	0.05	1.90	2.60
	0.05	225	0.20	4.40	2.40
	0.1	265	1.15	4.80	1.60
$\dot{q}_4(\omega = 0)$	0.005	370	0.30	2.50	2.10
	0.01	510	0.25	2.50	2.20
	0.05	405	1.85	4.30	1.90
	0.1	580	2.50	4.70	1.90

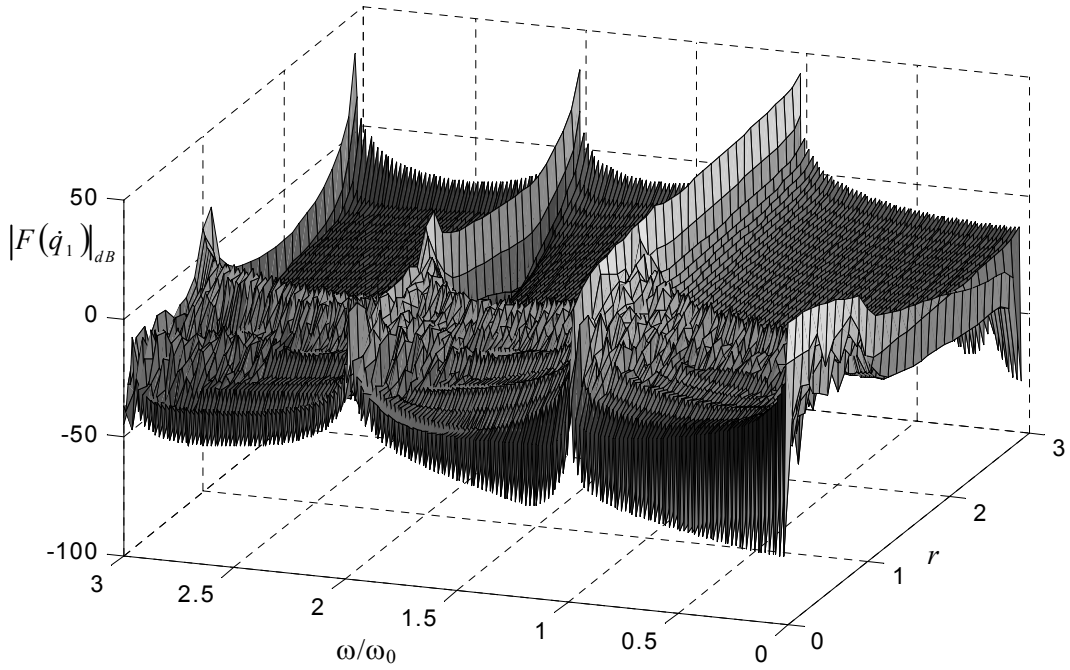

Figure 17 Fourier transform of the 3*R* robot joint 1 velocity, for 500 cycles, *vs* the radial distance *r* and the frequency ratio ω/ω_0, for $\rho = 0.1$ *m*, $\omega_0 = 3$ *rad/sec*.

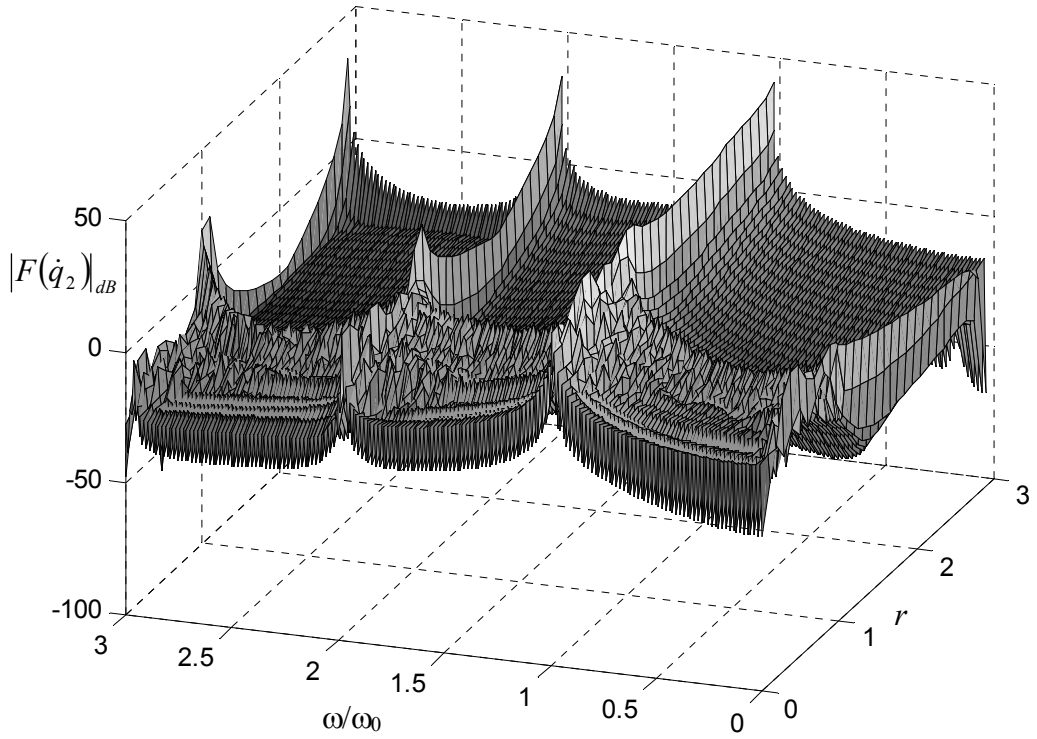

Figure 18 Fourier transform of the 3*R* robot joint 2 velocity, for 500 cycles, *vs* the radial distance *r* and the frequency ratio ω/ω_0, for $\rho = 0.1$ *m*, $\omega_0 = 3$ *rad/sec*.

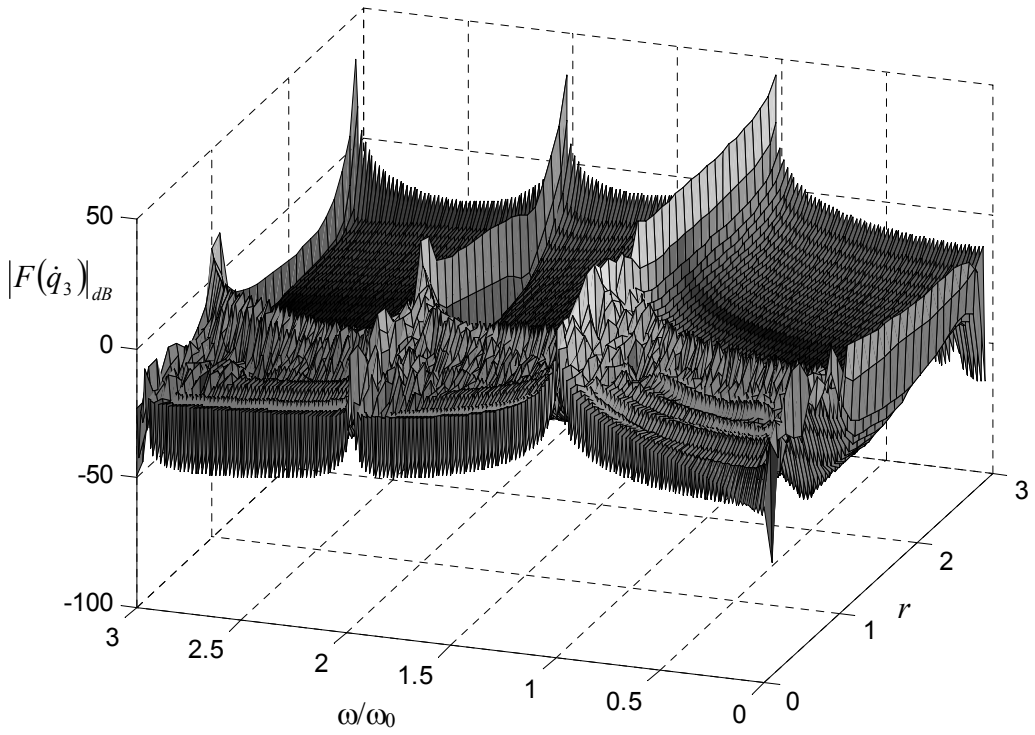

Figure 19 Fourier transform of the 3*R* robot joint 3 velocity, for 500 cycles, *vs* the radial distance *r* and the frequency ratio ω/ω_0, for $\rho = 0.1$ *m*, $\omega_0 = 3$ *rad/sec*.

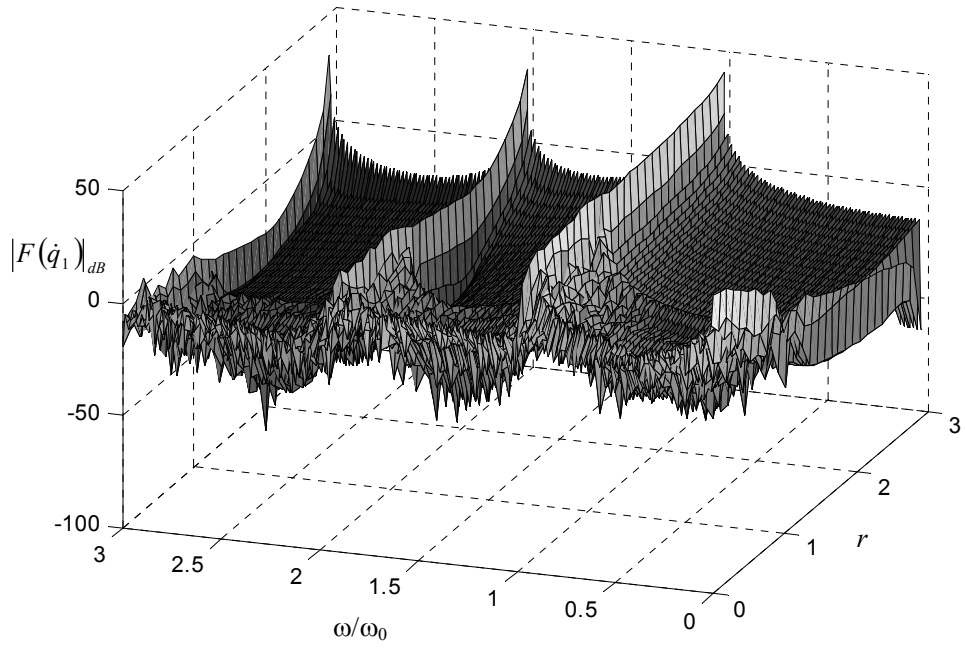

Figure 20 Fourier transform of the 4*R* robot joint 1 velocity, for 500 cycles, *vs* the radial distance *r* and the frequency ratio ω/ω_0, for $\rho = 0.1$ *m*, $\omega_0 = 3$ *rad/sec*.

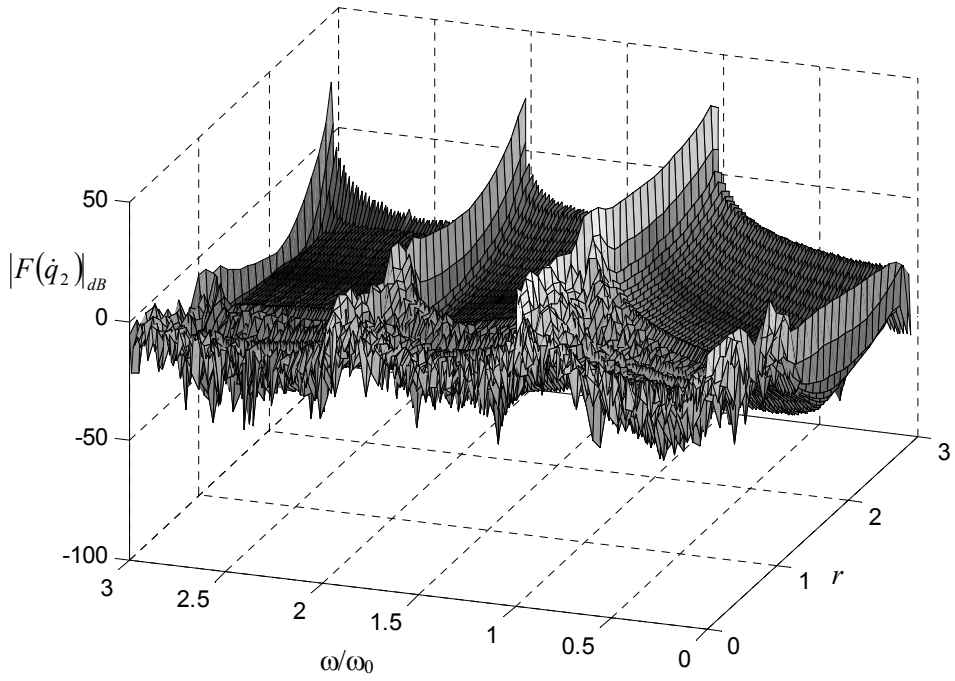

Figure 21 Fourier transform of the 4*R* robot joint 2 velocity, for 500 cycles, *vs* the radial distance *r* and the frequency ratio ω/ω_0, for $\rho = 0.1$ *m*, $\omega_0 = 3$ *rad/sec*.

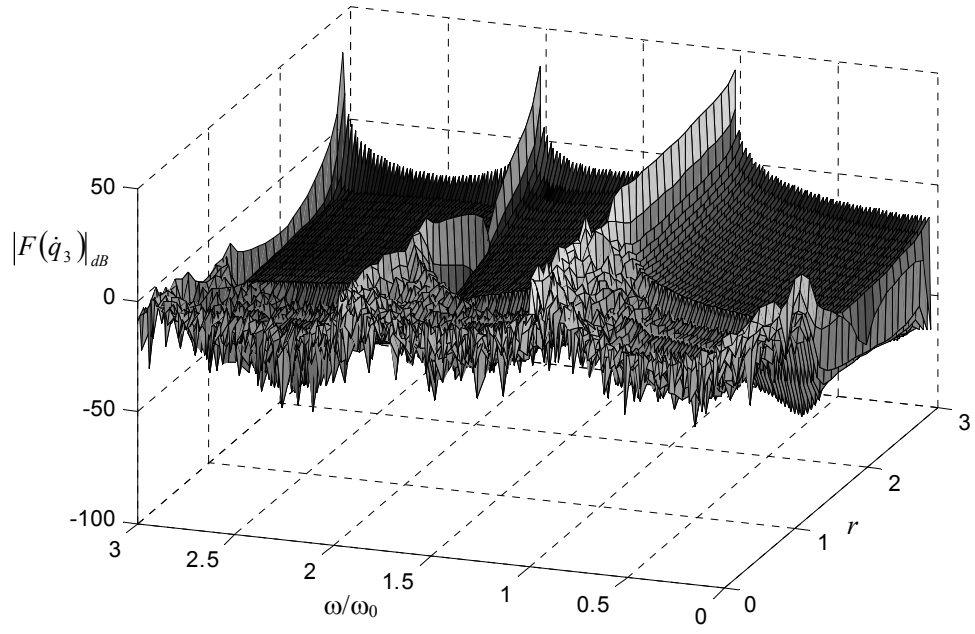

Figure 22 Fourier transform of the 4*R* robot joint 3 velocity, for 500 cycles, *vs* the radial distance *r* and the frequency ratio ω/ω_0, for $\rho = 0.1$ *m*, $\omega_0 = 3$ *rad/sec*.

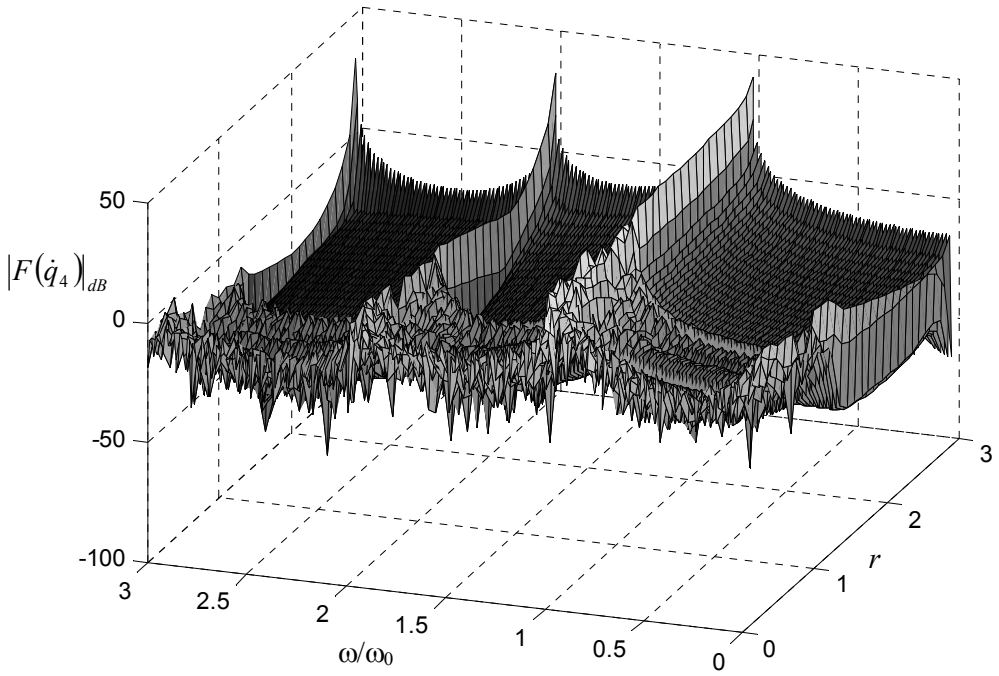

Figure 23 Fourier transform of the 4*R* robot joint 4 velocity, for 500 cycles, *vs* the radial distance *r* and the frequency ratio ω/ω_0, for $\rho = 0.1$ *m*, $\omega_0 = 3$ *rad/sec*.

Based on these results we conclude that the velocity drift changes with the robot end-effector radial distance *r*. Furthermore, the DC component is "induced" by the repetitive motion with a quadratic-like dependence with ρ.

5. Conclusions

This paper discussed several aspects of the phenomena generated by the pseudoinverse-based trajectory control of redundant manipulators.

The CLP scheme leads to non-optimal responses, both for the manipulability and the repeatability. Bearing these facts in mind, the fractal dimension of the responses was analyzed showing that it is independent of the robot joint. In fact, the chaotic motion depends on the point in the operational space and on the amplitude of the exciting repetitive motion. In this perspective, the chaotic responses were analyzed from different point of views namely, phase-plane, statistics and frequency response. The chaos revealed a fractional-order dynamics representative of the non-repetitive signals time history in contrast with the standard perspective that focus "local" phenomena represented by integer-order models. The results are consistent and represent a step towards the

development of superior trajectory planning algorithms for redundant and hyper-redundant manipulators.

Based on this study future developments will address the generalization to non-planar robots, the establishment of algorithms to avoid or to control chaos and the establishment of a deeper knowledge on the nature of phenomena with fraction-order dynamics.

References

1. Podlubny, I., *Fractional Differential Equations*, Academic Press, New York, 1999.

2. Gemant, A., 'On fractional differentials', *Philosophical Magazine* **25**, 1938, 540-549.

3. Oldham, K. B. and Spanier, J., *The Fractional Calculus: Theory and Application of Differentiation and Integration to Arbitrary Order*, Academic Press, New York, 1974.

4. Ross, B., 'Fractional Calculus', *Mathematics Magazine* **50(3)**, 1977, 15-122.

5. Oustaloup, A., *La Dérivation Non Entier:Théorie, Synthèse et Applications*, Hermes 1995.

6. Samko, S. G., Kilbas, A. A. and Marichev, O. I., *Fractional Integrals and Derivatives: Theory and Applications*, Gordon and Breach, New York, 1993.

7. Miller, K. S. and Ross, B., *An Introduction to the Fractional Calculus and Fractional Differential Equations*, Wiley, New York, 1993.

8. Osler, T. J., 'Leibniz rule for fractional derivatives generalized and its application to infinite series', *SIAM Journal of Applied Mathematics* **18(3)**, 1970, 658-674.

9. Osler, T. J., 'Taylor's series generalized for fractional derivatives and applications', *SIAM Journal of Mathematics Analysis* **2(1)**, 1971, 37-48.

10. Ross, B., 'Fractional calculus and its applications', in *Lecture Notes in Mathematics 457*, Springer-Verlag, New York, 1974.

11. Nishimoto, K., *Fractional Calculus (Volume IV): Integrations and Differentiations of Arbitrary Order*, Descartes Press, Japan, 1991.

12. Samko, S. G., 'Fractional integration and differentiation of variable order', *Analysis Mathematica* **21**, 1995, 213-236.

13. Campos, L. M. C., 'Fractional calculus of analytic and branched functions', in *Recent Advances in Fractional Calculus*, R. Kalia (eds), New York, 1993, 66-43.

14. Gemant, A.,'A method of analyzing experimental results obtained from elasto-viscous bodies', *Physics* **7**, 1936, 311-317.

15. Stiassnie, M., 'On the application of fractional calculus for the formulation of viscoelastic models', *Applied Mathematics Modelling* **3**, 1979, 300-302.

16. Bagley, R. L. and Torvik, P. J., 'Fractional calculus-a different approach to the analysis of viscoelastically damped structures', *AIAA Journal* **21(5)**, 1983, 741-748.

17. Rogers, L., 'Operators and fractional derivatves for viscoelastic constitutive equations', *Journal of Rheology* **27(4)**, 1983, 351-372.

18. Bagley, R. L. and Torvik, P. J., 'On the fractional calculus model of viscoelastic behaviour', *Journal of Rheology* **30(1)**, 1986, 133-155.

19. Koeller, R. C., 'Polynomial operators, stieltjes convolution, and fractional calculus in hereditary mechanics', *Acta Mechanica* **58**, 1986, 251-264.

20. Padovan, J., 'Computational algorithms for fe formulations involving fractional operators', *Computational Mechanics* **2(4)**, 1987, 271-287.

21. Koh, C. G. and Kelly, J. M., 'Application of fractional derivatives to seismic analysis of base-isolated models', *Earthquake Engineering and Structural Dynamics* **19**, 1990, 229-241.

22. Bagley, R. L. and Calico, R. A., 'Fractional order state equations for the control of viscoelastically damped structures', *ASME Journal of Guidance* **14(2)**, 1991, 304-311.

23. Makris, N., Constantinou, M. C. and Dargush, G. F., 'Analytical model of viscoelastic fluid dampers', *Journal of Structural Engineering* **119(11)**, 1993, 3310-3325.

24. Gaul, L. and Chen, C. M., 'Modeling of viscoelastic elastomer mounts in multibody systems', in *Advanced Multibody System Dynamics*, W. Schiehlen (eds), Kluwer Academic Publishers, Dordrecht,1993, 257-276.

25. Constantinou, M. C. and Symans, M. D., 'Experimental study of seismic response of buildings with supplemental fluid dampers', *The Structural Design of Tall Buildings* **2**, 1993, 93-132.

26. Gaul, L. and Schanz, M., 'Dynamics of viscoelastic solids treated by boundary element approaches in time domain', *European Journal of Mechanics, A/Solids* **13(4)**, 1994, 43-59.

27. Makris, N., Dargush, G. F. and Constantinou, M. C., 'Dynamic analysis of viscoelastic-fluid dampers', *Journal of Engineering Mechanics* **121(10)**, 1995, 1114-1121.

28. Fenander, Å., 'Modal synthesis when modelling damping by use of fractional derivatives', *AIAA Journal* **34(5)**, 1996, 1051-1058.

29. Liebst, B. S. and Torvik, P. J., 'Asymptotic approximations for systems incorporating fractional derivative damping', *ASME Journal of Dynamic Systems, Measurement, and Control* **118**, 1996, 572-579.

30. Clerc, J. P., Tremblay, A. M., Albinet, G. and Mitescu, C. D., 'A.C. response of fractal networks', *Le Journal de Physique-Lettres* **45(19)**, 1984, L.913-L.924.

31. Kaplan, T., Gray L. J. and Liu, S. H., 'Self-affine fractal model for a metal-electrolyte interface', *Physical Review* ***B*** **35(10)**, 1987, 5379-5381.

32. Méhauté, A. L., *Fractal Geometries: Theory and Applications*, Boca Raton, FL: CRC Press, 1992.

33. Anastasio, T. J., 'The fractional-order dynamics of brainstem vestibulo-oculomotor neurons', *Biological Cybernetics* **72**, 1994, 69-79.

34. Oustaloup, A., 'Fractional order sinusoidal oscillators: optimization and their use in highly linear fm modulation', *IEEE Transactions on Circuits and Systems* **28(10)**, 1981, 1007-1009.

35. Hosking, J. R. M., 'Fractional differencing', *Biometrika* **68(1)**, 1981, 165-176.

36. Ozaktas, H. M., Arikan, O., Kutay A. M. and Bozdagi, G., 'Digital computation of the fractional fourier transform', *IEEE Transactions on Signal Processing* **44(9)**, 1996, 2141-2150.

37. Ortigueira, M. D., 'Fractional discrete-time linear systems', *in Proceedings of the ICASSP'97-IEEE International Conference On Acoustics, Speech and Signal Processing*, Munich, Germany, April 20-24, 1997.

38. Dubois, D., Brienne, J. P., Pony, L. and Baussart, H., 'Study of a system described by an implicit derivative transmittance of non integer order with or without delay time', *in Proceedings of the IEEE-SMC/IMACS Symposium on Control, Optimization and Supervision*, Lille, France, 1996, pp. 826-830.

39. Nigmatullin, R. R., 'The realization of the generalized transfer equation in a medium with fractal geometry', *Physics of the State Solid (b)* **133**, 1986, 425-430.

40. Méhauté, A. L., Héliodore, F., Cottevieille, D. and Latreille, F., 'Introduction to wave phenomena and uncertainty in a fractal space', *Chaos, Solitons & Fractals* **3(5)**, 1993.

41. Mainardi, F., 'Fractional relaxation in anelastic solids', *Journal of Alloys and Compounds* **211/212**, 1994, 534-538.

42. Mainardi, F., 'Fractional relaxation-oscillation and fractional diffusion-wave phenomena', *Chaos, Solitons & Fractals* **7(9)**, 1996, 1461-1477.

43. Webman, I., 'Propagation and trapping of excitations on percolation clusters', *Journal of Statistical Physics* **6**, 1984, 603-614.

44. Matignon, D. and Anréa-Novel, B., 'Some results on controllability and observability of finite-dimensional fractional differential systems', in *Proceedings of the IEEE-SMC/IMACS Symposium on Control, Optimization and Supervision*, Lille, France, 1996, pp. 952-956.

45. Mathieu, B., Le Lay, L. and Oustaloup, A., 'Identification of non integer order systems in the time domain', *in Proceedings of the IEEE-SMC/IMACS Symposium on Control, Optimization and Supervision*, Lille, France, 1996, pp. 952-956.

46. Méhauté, A. L., 'From dissipative and to non-dissipative processes in fractal geometry: the janals', *New Journal of Chemistry* **14(3)**, 1990, 207-215.

47. Méhauté, A. L., 'Transfer processes in fractal media', *Journal of Statistical Physics* 36-**5/6**, 1984, 665-676.

48. Oustaloup, A., *La Commande CRONE: Commande Robuste d'Ordre Non Entier*, Hermes, Paris, 1991.

49. Oustaloup, A., Mathieu, B. and Lanusse, P., The CRONE control of resonant plants: Application to a flexible transmission', *European Journal of Control* **1(2)**, 1995, 113-121.

50. Tenreiro Machado, J. A., 'Analysis and design of fractional-order digital control systems', *SAMS - Journal Systems Analysis-Modelling-Simulation, Gordon & Breach Science Publishers* **28**, 1997, 107-122.

51. Tenreiro Machado, J. A. and Azenha, A., 'Fractional-order hybrid control of robot manipulators', *in Proceedings of the SMC'98-1998 IEEE International Conference on Systems, Man and Cybernetics*, San Diego, California, USA, 1998, pp. 788-793.

52. Tenreiro Machado, J. A., 'Discrete-time fractional-order controllers', *FCAA - Journal of Fractional Calculus & Applied Analysis* **4(1)**, 2001, 47-66.

53. Vinagre, B. M., Petras, I., Merchan, P.and Dorcak, L., 'Two digital realizations of fractional controllers: Application to temperatures control of a solid', *in Proceedings of the European Conference Control' 2001*, Porto, Portugal, 2001, pp. 1764-1767.

54. Podlubny, I., 'Fractional-order systems and $PI^{\lambda}D^{\mu}$ controllers', *IEEE Transactions on Automatic Control* **44(1)**, 1999, 208-213.

55. Ben-Israel, A. and Greville, T., *Generalized Inverses: Theory and Applications*, Wiley, New York, 1974.

56. Rao, C. R. and Mitra, S. K., *Generalized Inverse of Matrices and its Applications*, Wiley, New York, 1971.

57. Campbell, S. L. and Meyer, C. D., *Generalized Inverses of Linear Transformations*, Dover Publications, New York, 1979.

58. Goldberg, J. L., *Matrix Theory with Applications*, McGraw-Hill., New York, 1992.

59. Chiaverini, S., 'Singularity-robust task-priority redundancy resolution for real time kinematic control of robot manipulators', *IEEE Transactions Robotics Automation* **13**, 1997, 398-410.

60. Chung, W. J., Youm, Y. and Chung, W. K., 'Inverse kinematics of planar redundant manipulators via virtual links with configuration index', *Journal of Robotic Systems* **11**, 1994, 117-128.

61. Conkur, E. S. and Buckingham, R., 'Clarifying the definition of redundancy as used in robotics', *Robotica* **15**, 1997, 583-586.

62. Doty, K. L., Melchiorri, C. and Bonivento, C., 'A theory of generalized inverses applied to robotics', *Int.*, *Journal of Robotics Research* **12**, 1993, 1-19.

63. Yoshikawa, T., *Foundations of Robotics: Analysis and Control*, MIT Press, Massachusetts, 1988.

64. Duarte, F. B. and Tenreiro Machado, J. A., 'Kinematic optimazition of redundant and hyper-redundant robot trajectories', *in Prodeedings of the ICECS'98-5th IEEE International Conference on Electronics, Circuits and Systems*, Lisbon, Portugal, 1998.

65. Duarte, F. B. and Tenreiro Machado, J. A., 'On the optimal configuration of redundant manipulators', *in Proceedings of the INES'98- 9th IEEE Int. Conf. on Intelligent Engineering Systems*, Vienna, Austria, 1998.

66. Duarte, F. B. and Tenreiro Machado, J. A., 'Chaotic phenomena and performance optimization in the trajectory control of redundant manipulators' in *Recent Advances in Mechatronics*, O. Kaynak et al. (eds.), Springer-Verlag, New York, 1999.

67. Duarte, F. B. and Tenreiro Machado, J. A., 'Chaos dynamics in the trajectory control of redundant manipulators', *in Proceedings of the IEEE International Conference on Robotics and Automation*, S. Francisco, USA, 2000.

68. Klein, C. A. and Huang, C. C., 'Review of pseudoinverse control for use with kinematically redundant manipulators', *IEEE Transactions Systems, Man and Cyber*netics **13,** 1983, 245-250.

69. Tenreiro Machado, J. A. and Duarte, F. B., 'Redundancy optimization for mechanical manipulators', *in Proceedings of the 5th IEEE International Workshop on Advanced Motion Control,* Coimbra, Portugal*,* 1998.

70. Duarte, F. B. and Tenreiro Machado, J. A., 'Kinematic optimization of redundant and hyper-redundant robot trajectories', *in Proceedings of the ICECS'98-5th IEEE International Conference on Electronics, Circuits and Systems*, Lisbon, Portugal, 1998.

71. Duarte, F. B. and Tenreiro Machado, J. A., 'On the optimal configuration of redundant manipulators', *in Proceedings of the INES'98- 9th IEEE Int. Conf. on Intelligent Engineering Systems*, Vienna, Austria, 1998.

72. Nakamura, Y., *Advanced Robotics: Redundancy and Optimization*, Addison-Wesley, New York, 1991.

73. Roberts, R. G. and Maciejewski, A. A., 'Repeatble generalized inverse control strategies for kinematically redundant manipulators', *IEEE Transactions on Automatic Control* **38(5)**, 1993, 689-699.

74. Seereeram, S. and Wen, J. T., 'A global approach to path planning for redundant manipulators', *IEEE Transactions Robotics Automation* **11**, 1995, 152-159.

75. Siciliano, B., 'Kinematic control of redundant robot manipulators: A tutorial', *Journal of Intelligent and Robotic Systems* **3**, 1990, 201-212.

76. Theiler, J.,'Estimating fractal dimension', *Journal Optical Society of America* **7(6)**, 1990, 1055-1073.

77. Seereeram, S. and Wen, J. T., 'A global approach to path planning for redundant manipulators', *IEEE Transactions Robotics Automation* **11**, 1995, 152-159.

78. Roberts, R. G. and Maciejewski, A. A., 'Singularities, stable surfaces and the repeatable behaviour of kinematically redundant manipulators', *International Journal of Robotics Research* **13(1)**, 1994, 70-81.

79. Bay, J. S., 'Geometry and prediction of drift-free trajectories for redundant machines under pseudoinverse control', *International Journal of Robotics Research* **11(1)**, 1992, 41-52.